Spectroscopic, EPR, X-ray structural, and DFT studies of the complex compound of N_4-donor ligand with copper(II)

İsmail Yılmaz[1], Nursel S. Acar[2], Simon J. Coles[3], and Abdurrahman Şengül[*4]

[1] Department of Chemistry, Faculty of Science Karabük University, 78050 Karabuk, Turkey
[2] Department of Chemistry, Faculty of Science, Ege University, 35100, Bornova, Izmir, Turkey
[3] UK National Crystallography Service, School of Chemistry, University of Southampton, Southampton, SO1 71BJ, United Kingdom
[5] Department of Chemistry, Faculty of Arts and Sciences, Zonguldak Bülent Ecevit University, 67100 Zonguldak, Turkey. E-mail: sengul@beun.edu.tr; Fax: +90 372 257 4181; Tel: + 90 372 291 1126

A new mononuclear neutral five-coordinate copper(II) coordination compound [Cu(L)(H_2O)] (**1**) (L = 6,6′-*bis*(*N*H-benzimidazol-2-yl)-2,2′-bipyridine) was synthesized and characterized by IR, UV-Vis, EPR and LC-MS (APCI) analysis. The crystal structure was also determined by X-ray crystallography. In **1**, the copper(II) center adopts a five-coordinate distorted square-pyramidal (SP) geometry in which the basal plane formed by four of the nitrogen atoms of the ligand while the apical position is occupied by the oxygen atom of the water molecule. The four Cu–N bond lengths are 1.987(4), 1.992(4), 2.020(5) and 2.027(4) Å, and the longest bond of the apical Cu–O_w is 2.234(4) Å. The ligand undergoes deprotonation upon coordination to the metal center and acts as a dianionic tetradentate chelate to form a neutral complex [CuN_4O]. The X-band EPR data of **1** are in agreement with the crystallographic data indicating a typical five-coordinate SP geometry. This geometry is also obtained by Density Functional Theory calculations. Time-dependent (TD) DFT calculations were used to shed light on the assignment and the nature of the electronic transitions observed in the UV−Vis spectrum. The calculated results are found to be consistent with the experimental data. Non-linear optical properties were also calculated by DFT calculations.

KEYWORDS Copper, EPR, tetradentate, bipyridine, benzimidazole, Density Functional Theory,

1 INTRODUCTION

The N-H functionality which involves H-bonding or deprotonation by the anion may lead to a modification of the UV-vis spectrum and a color change [2] . Benzimidazole derivatives have been explored in a diverse area such as in biochemistry, solar cells, polymers, and separation of lanthanides and actinides, etc. [8]. Although there are extensive studies on the tridentate 2,6-bis(NH-benzimidazol-2-yl)pyridine [8], the studies on the potentially tetradentate N_4-donor ligand, 6,6'-bis(NH-benzimidazol-2-yl)-2,2'-bipyridine (L) are very few. At first, Masa-aki Haga [9] has reported the synthesis and the crystal structure of platinum(II) with the N-methyl derivative of L, in which the complex cation consists of two platinum(II) ions surrounded by two tridentate ligands and linked by one of N-methylbenzimidazolyl groups in L each other. This is a unique coordination mode consisting of tridentate and monodentate combination due to the steric effect of the N-methyl groups present in the benzimidazole subunits. Masa-aki Haga and co-workers have reported the coordination compound of the tetradentate N_4-chelating 6,6'-bis(NH-benzimidazol-2-yl)-2,2'-bipyridine (L) ligand with ruthenium(II), $[Ru(L)Cl_2]$, and also the electrochemical properties and catalytic reactivity of this stable C_2-symmetrical octahedral complex [10] . The final study based on the electronic spectra, ZINDO analysis and Langmuir-Blodgett studies of *trans*-dichloro(6,6'-bis(N-dodecyl-benzimidazol-2-yl)-2,2'-bipyridine)ruthenium(II) was reported by Haga and et al in 2000 [11]. As emphasized above, most studies involving ruthenium(II) coordination compounds have focused on the electrochemical and spectroscopic properties in relation to acid-base chemistry. Benzimidazoles which exist in a tautomeric form can bind to a metal center as either the neutral form or deprotonated form, and also diverse coordination modes depending on the metal ion and the solvent system used. The benzimidazole-pyridine ring system can also provide potential supramolecular recognition sites for π–π aromatic stacking and hydrogen bonding supramolecular interactions involving the NH group as a donor and the N-heterocyclic bases as

acceptor to study the importance of the hydrogen bond network [7,8]. The N-H functionality which involves H-bonding or complete deprotonation by the anion may lead to a modification of the UV-vis spectrum and to a color change [2].

To explore the coordination chemistry of copper(II) with the N_4-chelating ligand as illustrated in Scheme 1, here we report the synthesis, single-crystal X-ray structure, EPR, and electronic spectra of the copper(II) complex. TD-DFT studies are also performed to understand the electronic structure and also the NLO properties of the novel compound.

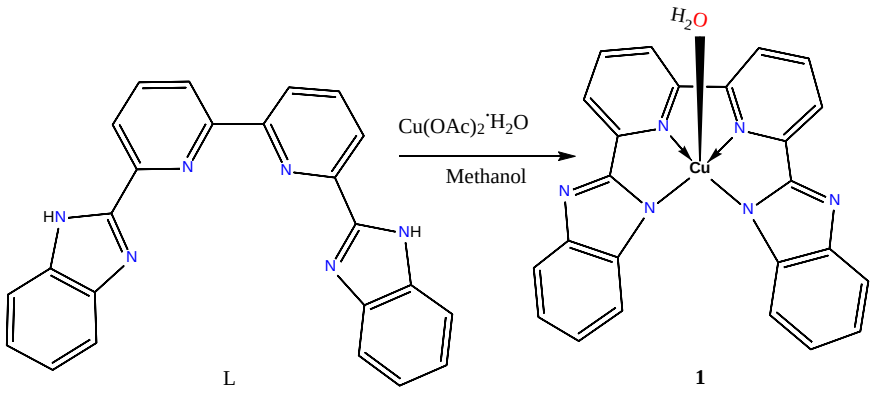

Scheme 1. Synthesis of the copper(II) complex, aqua-6,6′-bis(*N*H-benzimidazol-2-yl)-2,2′-bipyridylcopper(II), (**1**)

2 EXPERIMENTAL

2.1 Materials and instrumentation

All chemicals were obtained from commercial sources and used without further purification unless otherwise stated. Solvents were freshly distilled over appropriate drying reagents under dry N_2 atmosphere. Copper(II)-acetate salt was purchased from Merck. The synthesis of the ligand has been previously reported [10].

Infrared spectra were recorded on a Perkin-Elmer Spectrum 100 FT-IR spectrophotometer with an attenuated total reflection (ATR) accessory featuring a zinc selenide (ZnSe) crystal at room temperature. Electronic absorption spectra were measured on a CARY 100 Bio UV-Visible spectrophotometer in DMF solution at room temperature. MS analyses were performed by using LC\MS-API-ES, APCI: AGILENT 1100 MSD. The ESR spectrum was recorded on a Varian E-109C model X Band EPR spectrophotometer.

2.2 Synthesis of [Cu(L)(H_2O)] (1)

The ligand (0.05 g, 0.13 mmol) and $Cu(CH_3COO)_2{\cdot}H_2O$ (0.026g, 0.13 mmol) were dissolved in methanol (30 mL), and the mixture was stirred at 50-60 ºC for 3 h. The color of the solution turned green. After allowing the solution standing on the bench for a day, the resultant green precipitate was filtered and subsequently washed with plenty of diethyl ether and finally air-dried. It was recrystallized from the saturated DMF solution by slow evaporation at room temperature to afford green block crystals suitable for X-ray diffraction analysis. FT-IR [(ATR), cm^{-1}]: ν_{max}: 3051, 3017, 1667, 1601, 1575, 1510, 1452, 1398, 1367, 1323, 1265, 1229, 1166, 1149, 1092, 1077, 1069, 1021, 963, 875, 823, 800, 746, 737, 706, 653. UV-Vis (DMF at 25 °C): λ_{max} (nm) 325. APCI-MS **(*m/z*)**: 450.00 for $[M-H_2O]^+$ and 467.90 for $[M]^+$.

2.3 Crystal structure determination

Data collection was performed on a Nonius KappaCCD area detector (ϕ scans and ω scans to cover the asymmetric unit) at 120(2) K. The data collection was controlled by the COLLECT software [12]. The structure solution and refinement were performed using SHELX routines [13] from within the Olex2 software suite[14]. The details of data collection and crystal structure determination are gathered in Table 1. Crystallographic data for **1** have been deposited with the Cambridge Crystallographic Data Centre (CCDC deposition number1975175).

”TABLE 1”

2.4 Computational details

Optimizations in both gas phase and DMF were carried out by Gaussian09 [15] and Gaussview 5.0 [16] was used to visualize UV-Vis spectra and orbitals of the investigated molecules. Ground state calculations were carried out with DFT [17]. The B3LYP functional [18–20] was used for optimizations and CAM-B3LYP (includes long-range-correction terms) [21] was used for obtaining UV-Vis spectra in combination with the 6-31+G(d,p) and with LANL2DZ basis sets [22] (for Cu). Optimized structures were characterized as true minima with all positive values in frequency analyses. The first 100 singlet excited states of each system were taken into account in the TD-DFT calculations. Molecular orbital energies and UV-Vis spectra were obtained using optimized ground state geometries. Total electron density values for molecules was calculated using SCF density in all media. Solvent effects in the ground state were studied using the Polarizable Continuum Model (PCM) [23,24]. The nonlinear optical properties of the studied molecules were calculated according to the reference method [25].

3 RESULTS AND DISCUSSION

3.1 Synthesis and Characterization

The ligand, 6,6′-*bis*(*N*H-benzimidazol-2-yl)-2,2′-bipyridine (L) was prepared by a similar method previously reported by us [26] and others [10,11]. The ligand was characterized by MS (API-ES), ^{1}H and ^{13}C NMR spectroscopy. The characterization data were found to be identical with the reported data and are given in the supplementary material. The reaction between

[$Cu(CH_3COO)_2 \cdot H_2O$] and L in methanol provide the neutral complex [$Cu(L)(H_2O)$] (**1**). The complex is slightly soluble in methanol and very soluble in DMF and DMSO. The spectroscopic data of the complex are consistent with the proposed structure. The MS spectrum (Fig. S1) shows a minor peak at *m/z* 467.07 with a very low percentage due to labile water molecule in the mass experiment condition which confirms the presence of the coordinated water molecule in the complex. The peak at *m/z* 450.0 readily confirms the structure as $[M\text{-}H_2O]^+$. The Cu–O stretching frequency is usually observed in the low-frequency region at 440 cm^{-1} which is out of the detection limit of the instrument (Fig. S2), but the appearance of a band in the region 875 cm^{-1} can be assigned to the rocking mode of the coordinated water molecule [27,28] and is further confirmed by the X-ray studies (*vide infra*). It should be emphasized that the fundamental NH stretching band is not observed in the IR spectrum which further compromises with deprotonation of the coordinated ligand in the neutral complex (**1**). The X-band ESR spectrum of **1** at room temperature is shown in Fig. 1. The g_{II} and g_I values are 2.1294 and 2.0506, respectively indicating a five-coordinate SP geometry around the metal center [29].

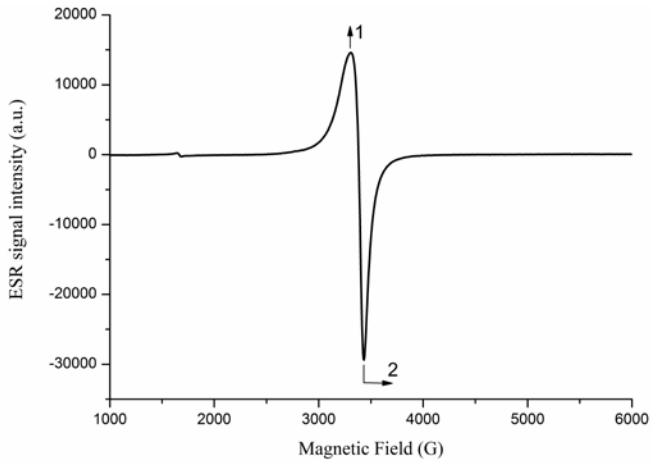

Figure 1. The X-band ESR spectrum of **1**

3.2 Description of the crystal structure of [$Cu(L)(H_2O)$] (1)

A diagram of **1** illustrating the atom labeling scheme is shown in Fig. 2. The copper(II) ion adopts a five-coordinate geometry in which the copper(II) ion coordinates to four N atoms of L-two benzimidazole (BI) N(1) and N(5) atoms and two 2,2′-bipyridine (BP) N(3) and N(4) atoms in the basal plane, and to an oxygen atom of the coordinated water in the fifth, apical position. The equatorial bond distances are nearly equal but due to the sterically more demanding BI, the Cu–$N_{(BP)}$ distances [1.992(4) and 1.987(4) Å] are slightly shorter than those of Cu–$N_{(BI)}$ [2.027(4) and 2.020(4) Å]. The ligand forms three sets of five-member chelate rings with the copper atom and their intra-ligand bite angles are 76.68(19)° [N(4)–Cu–N(3)], 79.85(18)° [N(3)–Cu–N(1)] and 80.33(19)° [N(4)–Cu–N(5)]. The Cu–O_w 2.234(4) Å is longer than the equatorial Cu–N distances as expected for the distorted square-pyramidal (SP) geometry, due to the effect of the chelate ring formed by the copper atom [29,30]. The apical Cu–O bond is nearly perpendicular [N–Cu–O angles 92.78(17)-98.10(16)°] to the N_4-equatorial plane. The bond distances and angles within the ligand are in the normal range. The *trans* angles N(3)–Cu–N(5) and N(4)–Cu–N(1) are 156.50(18) and 152.60(18)°, respectively as an indication of a distorted SP geometry. The mean planes of the two BI moieties intersect at 10.38°. These values reflect the net constraint at the metal upon coordination to the N_4-chelating ligand.

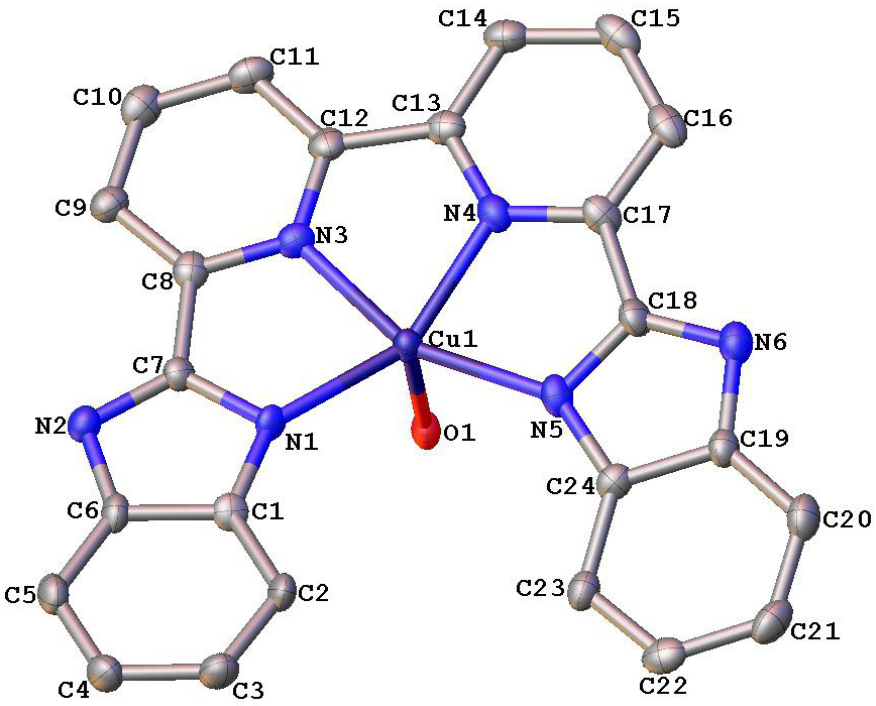

Figure 2. Molecular structure of **1** with the atom labeling scheme

The 'Tau Descriptor', τ, for five-coordinate compounds [30], calculated by the program PLATON [31], is 0.07 for **1** (extreme forms: τ = 0.00 for Square Pyramidal, SP, and 1.00 for a Trigonal Bipyramidal, TBP). The Berry Pseudo rotation coordinate for the D3h ···> C2v ···> C4v distortion is 79.1 and therefore the title complex is closest to C_{4v} symmetry and tends towards a distorted SP geometry.

The free ligand undergoes deprotonation upon coordination to copper(II) ion to form a five-membered chelate ring in similar to other analogous ligands (i.e. 2(2′-pyridyl)benzimidazole) [32]. The bond distances in the ligand are in the expected range [7].

In the crystal lattice, the neutral molecule forms hydrogen bonds via BI tertiary N atoms as an acceptor and the apical water molecules as the donor. Each water molecule hydrogen bonds with the adjacent molecules above the mean plane (*b*-axis) through O–H···$N_{(BI)}$ and also from the water molecules of the adjacent molecules to BI N atoms through O–H···$N_{(BI)}$ to form

an infinite 1D-chain as shown in Fig.3. The BP and one of the BI planes are almost coplanar, but the other BI lies down the mean plane with an angle of 10.89°. This clearly shows the demanding steric nature of the bulky benzimidazole groups upon coordination to the metal center as a chelating ligand. The antiparallel molecular units are stacked to each other by 3.42 Å, generating significant π-π interactions that stabilize the crystal structure.

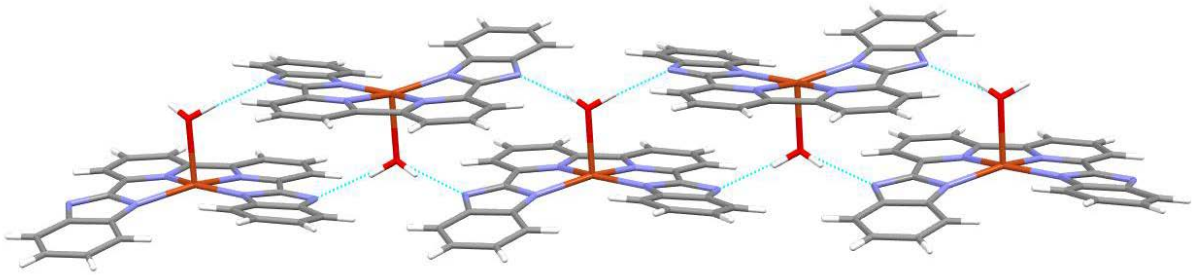

Figure 3. The hydrogen-bonding network formed in (**1**)

3. Theoretical investigations

The optimized structures of **1** for ground-state in the gas phase and DMF are given in Fig. S3 at B3LYP/6-31+G(d,p) level with LANL2DZ basis set on metals. The experimental and the calculated (in the gas phase) bond distances and bond angles were listed in Table S1 for comparison. The experimental and the calculated values are generally similar to the highest difference observed between O1-Cu1 atoms (nearly 0.2 Å). The differences between other atoms are about 0.04 Å. The computationally obtained values are usually slightly larger than the experimental values because the latter was measured in the solid phase where a molecule is surrounded by other molecules. On the other hand, a single molecule was investigated in the gas phase. As for the angles, the largest difference between the experimental and the computational values is 1.3°. Fig. S4 provides a better understanding of all the differences in distances and angles. The N3-Cu-N4 angle [76.68(19)°] is smaller than N1-Cu-N5

[120.86(18)°]. Due to the steric effects of hydrogens in the phenyl ring, it can cause deviation from the molecular planarity and distortion of SP geometry around the copper center.

Some of the selected parameters of the molecule calculated with B3LYP functionals including the sum of electronic energies with thermal free energies ($E_{elec}+\Delta G$) and total electronic energies with zero-point energy corrections (E_{elec}+ZPE, Hartree) in the gas phase and DMF are given in Table S2. When the dielectric constant of the medium increased, the dipole moment of the molecule is almost doubled and the molecule is more stable in the polar environment at 0 K and room temperature (negative ΔE and $\Delta\Delta G$).

Adiabatic and Vertical Ionization Potentials (AIP and VIP), and Adiabatic and Vertical Electron Affinities (AEA and VEA) are also calculated. Adiabatic Ionization Potentials (AIP) and Vertical Ionization Potentials (VIP) are calculated by using the neutral and the cationic forms. The energy difference between the neutral molecule (E_0) and the cation ($E.^*$) of the neutral molecule (VEA = $E.^* - E_0$) and between the neutral molecule and the cation in their most stable geometries (AEA = $E. - E_0$) are calculated, respectively (Table S3). VIP and AIP values are calculated as 8.01 eV and 7.66 eV, respectively. VEA and AEA values are also calculated as 2.01 eV and 2.94 eV, respectively. Similar values obtained for Vertical and Adiabatic values indicate that the molecular geometries are very similar in neutral, cationic and anionic forms.

Since Cu has an odd number of electrons (Cu^{II}, d^9 configuration), the SOMOs (single occupied molecular orbitals) are shown with α and β-spin (Figure 4). SOMO orbital energies are close for α and β-spins. However, the LUMO values of β orbitals are more negative compared to the α orbitals, resulting in a smaller SOMO-LUMO gap (ΔE_{S-L}). Electronic transitions are given according to β-spin electrons except for the cases where a major contribution comes from α-spin electrons.

	α-spin	β-spin
ΔE_{S-L} (eV)	**5.80**	**5.39**
LUMO	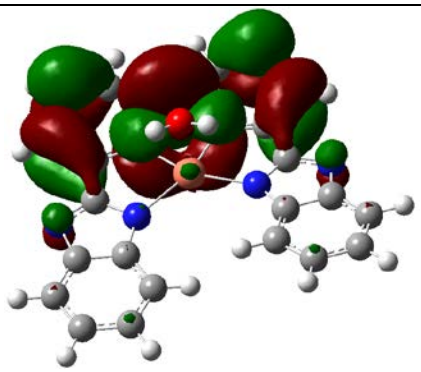	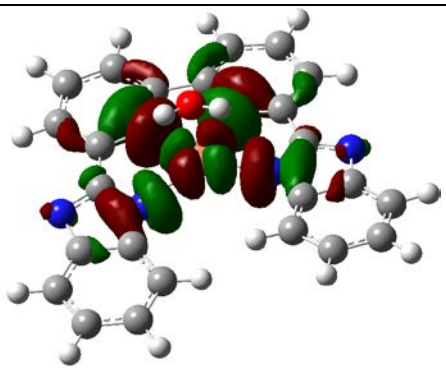
E_L (eV)	-1.50	-1.99
SOMO	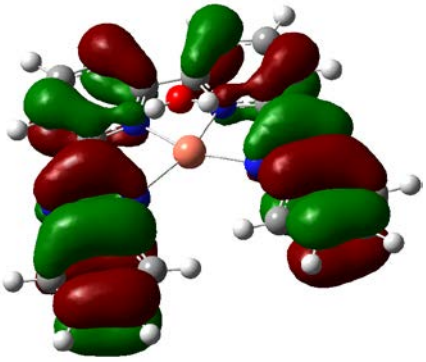	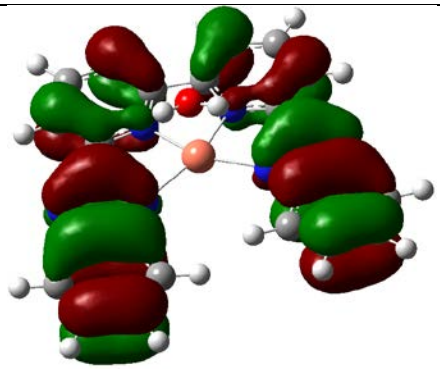
E_S (eV)	-7.30	-7.29

Fig. 4. SOMO-LUMO orbital energies (E_S, E_L) and energy gaps (ΔE_{S-L}) of investigated compound (**1**) at UCAM-B3LYP/6-31+G(d,p)/LANL2DZ level in DMF

B3LYP/6-31+G(d,p)/LANL2DZ and CAM-B3LYP/6-31+G(d,p)/LANL2DZ levels were used in TD-DFT calculations to obtain the absorption wavelengths and excitation energies for the first 100 singlet excited states (from S_0 to S_{100}). The CAM-B3LYP values are in better agreement with the experimental results in DMF (Fig. S5); thus, the following discussion is based on CAM-B3LYP/6-31G(d,p) results unless otherwise stated.

$S_0 \rightarrow S_1$ transition (722 nm in DMF) has intermolecular CT from water to Cu (CT1) and d-d transition. Additionally, it has intramolecular CT from BI and BP to Cu (CT2) and intramolecular CT from BI to Cu (CT3). S_2 transition displays similar transitions in addition to

ligand-to-metal CT from BI and BP to Cu moiety (LMCT). There are electronic transitions including metal up to transition S_7. Unfortunately, those transitions have very low oscillator strengths and could not be observed experimentally. S_7 (429 nm) and S_8 (421 nm) are local excitation for BI (LE2) and local excitation for BP (LE3) with π-π* character. Full LMCT transitions are observed at 390 nm, 290 nm, and 265 nm. The maximum peak at 331 nm displays an intramolecular CT from BI to BP and local excitation of BP with π-π* character (Fig. 5). There is also a CT from Cu to BI and BP (MLCT) with α-spin electron at 253 nm. Another different CT is named as CT5 (intramolecular charge-transfer from BP to BI) at 261 nm and contains π-π*, n-π* transitions.

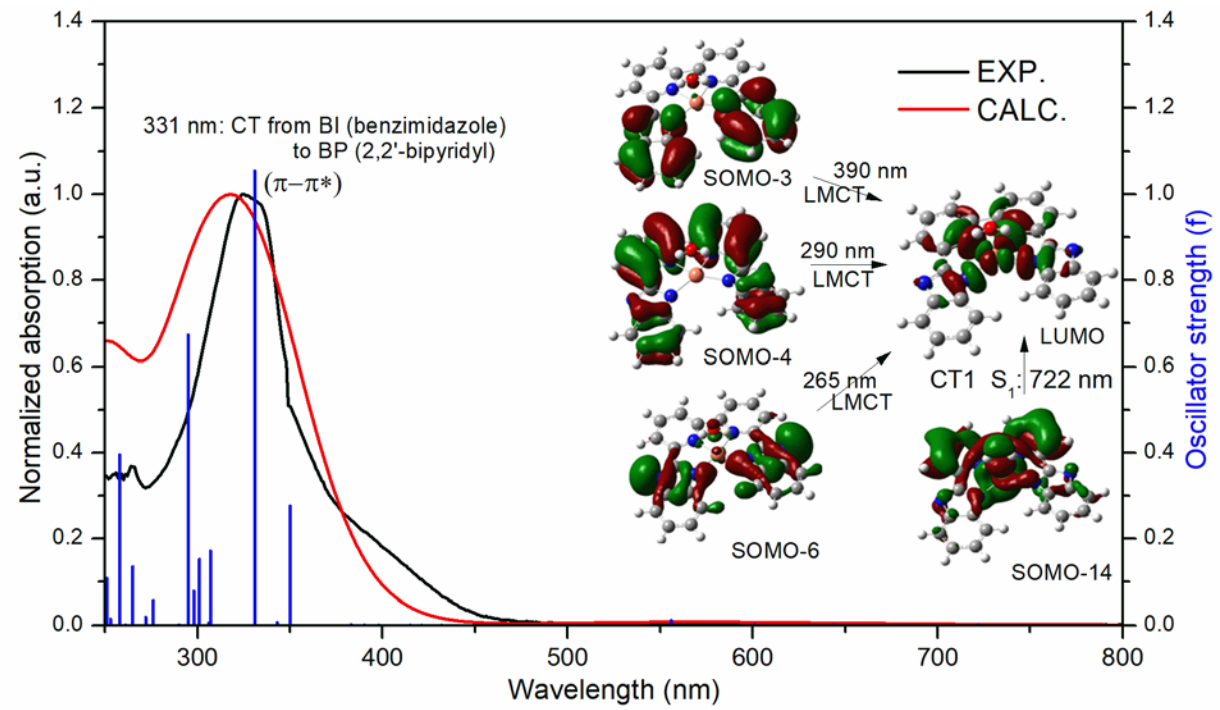

Fig. 5. The UV-Vis absorption spectra of **1** (with oscillator strength values) in DMF calculated at CAM-B3LYP/6-31+G(d,p) and LANL2DZ (for Cu) level

Nonlinear optical (NLO) materials provide useful properties for signal processing, optical switching, optical logic, and optical data storage and are currently driving

technological advances [33–35]. The molecular properties related to the nonlinear optical activity (NLO) can be obtained by the computational methods [25,36–42].

The polarizability α, the hyperpolarizability β and the electric dipole moment μ of **1**) is calculated using B3LYP/6-31+G(d,p)/LANL2DZ basis sets in the gas phase. Table 2 shows the total electric dipole moment (μ_{tot}), the mean polarizability (α_0), the anisotropy of the polarization (α_{tot}) and the first-order hyperpolarizability (β_{tot}). There are three important parameters for active NLO properties: higher values of dipole moment, molecular polarizability, and hyperpolarizability. The value of β_{tot} (62.28×10^{-30} esu) is 167 times larger than that of urea (0.37289×10^{-30} esu at B3LYP/6-31G(d)[43]) for **1**. These results indicate that **1** is a good candidate for NLO material.

TABLE 2

4 CONCLUSION

We report the single-crystal X-ray structure of **1,** in which a copper(II) center adopts a distorted square-pyramidal geometry via coordination to the N_4-ligand in the basal plane and the water molecule in the apical position. The ligand undergoes deprotonation upon coordination to the metal center and acts as a dianionic ligand. The EPR spectrum further supports the distorted SP geometry of $[Cu(N_4)O]$ which is consistent with the $d_{x^2-y^2}$ ground state. DFT computations revealed that the compound has a significant non-linear optical activity, most probably due to extensive metal center-ligand charge-transfer process.

Supporting Information

The supporting information includes FT-IR, UV-Vis and MS mass of 1. The supplementary crystallographic data for CCDC 1975175 (**1**) can be obtained free of charge via http://www.ccdc.cam.ac.uk/conts/retrieving.html (or from the Cambridge Crystallographic Data Centre, 12, Union Road, Cambridge CB2 1EZ, UK; fax: +44 1223 336033).

Acknowledgments

This work was supported by the Turkish Scientific and Technical Research Council (TÜBİTAK) [TBAG-2450, grant number 111T062]. Computer time provided on FenCluster by Faculty of Science, Ege University and on TUBITAK-ULAKBIM TRUBA resources are gratefully acknowledged.

Conflicts of Interest: The authors declare no conflict of interest

REFERENCES

[1] S. Tahlan, S. Kumar, B. Narasimhan, Pharmacological significance of heterocyclic 1H-benzimidazole scaffolds: a review, BMC Chem. 13 (2019) 1–21. doi:10.1186/s13065-019-0625-4.

[2] D. Udhayakumari, Chromogenic and fluorogenic chemosensors for lethal cyanide ion. A comprehensive review of the year 2016, Sensors Actuators, B Chem. 259 (2018) 1022–1057. doi:10.1016/j.snb.2017.12.006.

[3] Y.C. Wu, J.Y. You, K. Jiang, H.Q. Wu, J.F. Xiong, Z.Y. Wang, Novel benzimidazole-based ratiometric fluorescent probes for acidic pH, Dye. Pigment. 149 (2018) 1–7. doi:10.1016/j.dyepig.2017.09.043.

[4] H.J. Kim, C.H. Heo, H.M. Kim, Benzimidazole-based ratiometric two-photon fluorescent probes for acidic pH in live cells and tissues, J. Am. Chem. Soc. 135 (2013) 17969–17977. doi:10.1021/ja409971k.

[5] Z. Li, L.J. Li, T. Sun, L. Liu, Z. Xie, Benzimidazole-BODIPY as optical and fluorometric pH sensor, Dye. Pigment. 128 (2016) 165–169. doi:10.1016/j.dyepig.2016.01.029.

[6] E. Horak, M. Hranjec, R. Vianello, I.M. Steinberg, Reversible pH switchable aggregation-induced emission of self-assembled benzimidazole-based acrylonitrile dye in aqueous solution, Dye. Pigment. 142 (2017) 108–115. doi:10.1016/j.dyepig.2017.03.021.

[7] A. Sengul, I. Yilmaz, N. Karadayi, S.J. Coles, Spectroscopic and structural studies of 6-(1-methylbenzimidazol-2-yl)-1H- pyridin-2-one and of an unusual T4(2)7(2)6(2)7(2) water tape stabilized by the copper(II) coordination polymer, Inorganica Chim. Acta. 370 (2011) 369–373. doi:10.1016/j.ica.2011.02.010.

[8] M. Boča, R.F. Jameson, W. Linert, Fascinating variability in the chemistry and properties of 2,6-bis-(benzimidazol-2-yl)-pyridine and 2,6-bis-(benzthiazol-2-yl)-pyridine and their complexes, Coord. Chem. Rev. 255 (2011) 290–317. doi:10.1016/j.ccr.2010.09.010.

[9] M. Haga, K. Hiratsuka, M. Kato, H. Kurosaki, M. Goto, R. Arakawa, S. Yano, Self-assembled Dinuclear Platinum (II) Complexes with 6, 6′-Bis (1-methylbenzimidazol-2-yl)-2, 2′-bipyridine: Synthesis, X-Ray Structure, and Solution Behaviors, Chem. Lett. 24 (1995) 1143–1144.

[10] K. Mizushima, M. Nakaura, S. Park, H. Nishiyama, H. Monjushiio, K. Harada, M.

Haga, Ruthenium (II) complexes with the tetradentate 6 , 6 ’ -bis (oxazolinyl or properties , and catalytic reactivities, Synthesis (Stuttg). 261 (1997) 175–180.

[11] M.F. Ryan, R. a. Metcalfe, A.B.P. Lever, M. Haga, A novel ruthenium surfactant: electronic spectra, ZINDO analysis and Langmuir–Blodgett studies of trans-dichloro(6,6′-bis(N-dodecylbenzimidazol-2-yl)-2,2′-bipyridine)ruthenium(II)†, J. Chem. Soc. Dalt. Trans. (2000) 2357–2366. doi:10.1039/b002123g.

[12] R.W.W. Hooft, Collect, Nonius BV, Delft, Netherlands. (1998).

[13] G.M. Sheldrick, Crystal structure refinement with SHELXL, Acta Crystallogr. Sect. C Struct. Chem. 71 (2015) 3–8. doi:10.1107/S2053229614024218.

[14] O. V Dolomanov, L.J. Bourhis, R.J. Gildea, J.A.K. Howard, H. Puschmann, OLEX2: a complete structure solution, refinement and analysis program, J. Appl. Crystallogr. 42 (2009) 339–341.

[15] M.J. Frisch, G.W. Trucks, H.B. Schlegel, G.E. Scuseria, M.A. Robb, J.R. Cheeseman, G. Scalmani, V. Barone, B. Mennucci, G.A. Petersson, H. Nakatsuji, M. Caricato, X. Li, H.P. Hratchian, A.F. Izmaylov, J. Bloino, G. Zheng, J.L. Sonnenberg, M. Hada, M. Ehara, K. Toyota, R. Fukuda, J. Hasegawa, M. Ishida, T. Nakajima, Y. Honda, O. Kitao, H. Nakai, T. Vreven, J.A. Montgomery, Jr., J.E. Peralta, F. Ogliaro, M. Bearpark, J.J. Heyd, E. Brothers, K.N. Kudin, V.N. Staroverov, R. Kobayashi, J. Normand, K. Raghavachari, A. Rendell, J.C. Burant, S.S. Iyengar, J. Tomasi, M. Cossi, N. Rega, J.M. Millam, M. Klene, J.E. Knox, J.B. Cross, V. Bakken, C. Adamo, J. Jaramillo, R. Gomperts, R.E. Stratmann, O. Yazyev, A.J. Austin, R. Cammi, C. Pomelli, J.W. Ochterski, R.L. Martin, K. Morokuma, V.G. Zakrzewski, G.A. Voth, P. Salvador, J.J. Dannenberg, S. Dapprich, A.D. Daniels, Ö. Farkas, J.B. Foresman, J.V.

Ortiz, J. Cioslowski and D.J. Fox, Gaussian 09 C.01, Gaussian, Inc. Wallingford CT. (2009).

[16] R.D. Dennington, T.A. Keith, J.M. Millam, others, GaussView 5.0. 8, Gaussian Inc. 340 (2008).

[17] W. Kohn, L.J. Sham, Self-consistent equations including exchange and correlation effects, Phys. Rev. 140 (1965) A1133.

[18] A.D. Becke, Density-functional exchange-energy approximation with correct asymptotic behavior, Phys. Rev. A. 38 (1988) 3098-3100.

[19] A.D. Becke, Becke's three parameter hybrid method using the LYP correlation functional, J. Chem. Phys. 98 (1993) 5648–5652.

[20] C. Lee, W. Yang, R.G. Parr, Development of the Colle-Salvetti correlation-energy formula into a functional of the electron density, Phys. Rev. B. 37 (1988) 785-789.

[21] T. Yanai, D.P. Tew, N.C. Handy, A new hybrid exchange--correlation functional using the Coulomb-attenuating method (CAM-B3LYP), Chem. Phys. Lett. 393 (2004) 51–57.

[22] T.H. Dunning, P.J. Hay, Methods of electronic structure theory, in: Mod. Theor. Chem., Plenum Press New York, 1977: p. 1-28.

[23] J. Tomasi, B. Mennucci, E. Cances, The IEF version of the PCM solvation method: an overview of a new method addressed to study molecular solutes at the QM ab initio level, J. Mol. Struct. THEOCHEM. 464 (1999) 211–226.

[24] J. Tomasi, B. Mennucci, R. Cammi, Quantum mechanical continuum solvation models,

Chem. Rev. 105 (2005) 2999–3094.

[25] D. Sajan, H. Joe, V.S. Jayakumar, J. Zaleski, Structural and electronic contributions to hyperpolarizability in methyl p-hydroxy benzoate, J. Mol. Struct. 785 (2006) 43–53.

[26] A. Şengül, Ö. Kurt, P.D.F. Adler, S.J. Coles, Spectroscopic and structural properties of complexes of 3,3′-bis(2-benzimidazolyl)-2,2′-bipyridine with copper(i) and silver(i), J. Coord. Chem. 67 (2014) 2365–2376. doi:10.1080/00958972.2014.943201.

[27] G.T. Behnke, K. Nakamoto, Infrared Spectra and Structure of Acetylacetonato Platinum(II) Complexes. I. Infrared Spectra and Normal Coordinate Analysis of Potassium Dichloro(Acetylacetonato)Platinate(II), Inorg. Chem. 6 (1967) 433–440. doi:10.1021/ic50049a001.

[28] K. Gudasi, R. Vadavi, R. Shenoy, M. Patil, S.A. Patil, M. Nethaji, Transition metal complexes of a tridentate ligand bearing two pendant pyridine bases: The X-ray crystal structure of pentacoordinate copper(II) complex, Inorganica Chim. Acta. 358 (2005) 3799–3806. doi:10.1016/j.ica.2005.07.033.

[29] M.H. Sadhu, S.B. Kumar, Synthesis, characterization and structures of copper(II) and cobalt(II) complexes involving N3S-coordinated tetradentate ligand and azide/ thiocyanate/ nitrite ion, J. Mol. Struct. 1164 (2018) 239–247. doi:10.1016/j.molstruc.2018.03.040.

[30] D. Trans, A.W. Addison, T.N. Rao, Synthesis, Structure, and Spectroscopic Properties, (1984).

[31] A.L. Spek, PLATON, molecular geometry program, J. Appl. Crystallogr. 36 (2003).

[32] L.J. Chen, X. He, Q.Z. Zhang, X.Y. Wu, C. zhong Lu, A new one-dimensional copper-

molybdenum bimetallic oxide compound with coordinated 2-PBIM: [Cu(2-PBIM)MoO4] (2-PBIM = 2-(2-pyridyl)benzimidazole), Inorg. Chem. Commun. 9 (2006) 740–743. doi:10.1016/j.inoche.2006.04.019.

[33] C. Andraud, T. Brotin, C. Garcia, F. Pelle, P. Goldner, B. Bigot, A. Collet, Theoretical and experimental investigations of the nonlinear optical properties of vanillin, polyenovanillin, and bisvanillin derivatives, J. Am. Chem. Soc. 116 (1994) 2094–2102.

[34] M. Nakano, H. Fujita, M. Takahata, K. Yamaguchi, Theoretical study on second hyperpolarizabilities of phenylacetylene dendrimer: Toward an understanding of structure- property relation in NLO responses of fractal antenna dendrimers, J. Am. Chem. Soc. 124 (2002) 9648–9655.

[35] V.M. Geskin, C. Lambert, J.-L. Brédas, Origin of high second-and third-order nonlinear optical response in ammonio/borato diphenylpolyene zwitterions: the remarkable role of polarized aromatic groups, J. Am. Chem. Soc. 125 (2003) 15651–15658.

[36] A. Karaka\cs, A. Elmali, H. Ünver, I. Svoboda, Nonlinear optical properties, synthesis, structures and spectroscopic studies of N-(4-nitrobenzylidene)-o-fluoroamine and N-(3-nitrobenzylidene)-p-fluoroamine, Spectrochim. Acta Part A Mol. Biomol. Spectrosc. 61 (2005) 2979–2987.

[37] P.S. Liyanage, R.M. de Silva, K.M.N. de Silva, Nonlinear optical (NLO) properties of novel organometallic complexes: high accuracy density functional theory (DFT) calculations, J. Mol. Struct. THEOCHEM. 639 (2003) 195–201. doi:10.1016/J.THEOCHEM.2003.08.009.

[38] P.J. Mendes, J.P.P. Ramalho, A.J.E. Candeias, M.P. Robalo, M.H. Garcia, Density

functional theory calculations on $η$5-monocyclopentadienylnitrilecobalt complexes concerning their second-order nonlinear optical properties, J. Mol. Struct. THEOCHEM. 729 (2005) 109–113.

[39] H. Alyar, Z. Kantarci, M. Bahat, E. Kasap, Investigation of torsional barriers and nonlinear optical (NLO) properties of phenyltriazines, J. Mol. Struct. 834 (2007) 516–520.

[40] I.C. de Silva, R.M. de Silva, K.M.N. De Silva, Investigations of nonlinear optical (NLO) properties of Fe, Ru and Os organometallic complexes using high accuracy density functional theory (DFT) calculations, J. Mol. Struct. THEOCHEM. 728 (2005) 141–145.

[41] J.O. Morley, Nonlinear optical properties of organic molecules. 7. Calculated hyperpolarizabilities of azulenes and sesquifulvalene, J. Am. Chem. Soc. 110 (1988) 7660–7663.

[42] H. Li, K. Han, X. Shen, Z. Lu, Z. Huang, W. Zhang, Z. Zhang, L. Bai, The first hyperpolarizabilities of hemicyanine cationic derivatives studied by finite-field (FF) calculations, J. Mol. Struct. THEOCHEM. 767 (2006) 113–118. doi:10.1016/J.THEOCHEM.2006.05.008.

[43] C. Adant, M. Dupuis, J.L. Bredas, Ab initio study of the nonlinear optical properties of urea: Electron correlation and dispersion effects, Int. J. Quantum Chem. 56 (1995) 497–507. doi:10.1002/qua.560560853.

Table 1. Crystal structure refinement and data collection parameters for **1**

	(**1**)
Formula	C24H16CuN6O
Formula Weight	467.97
Crystal System	monoclinic
Space Group	$P2_1/c$
a /Å	11.1475(5)
b /Å	17.9969(8)
c /Å	10.2634(5)
β /°	105.017(3)
V /Å^3	1988.73(16)
Z	4
$D_{c.}$ /g cm^{-3}	1.563
Crystal size /mm	0.16 × 0.03 × 0.01
Crystal colour	yellow
Crystal shape	shard
Wavelength /Å	0.71073
Radiation type	MoK$_\alpha$
μ /mm^{-1}	1.130
T /K	120(2)
hkl range	$-14 \le h \le 13$, $-23 \le k \le 23$, $-13 \le l \le 13$
Independent Refl.	4550
Reflections with [$I > 2\sigma(I)$]	3087
No. of parameters	297
R_{int}	0.1116
R_1 (F) [$I > 2\sigma(I)$]	0.0745
wR_2 (F^2)	0.1511
Goodness-of-fit	1.108
$\Delta\rho_{mim;max}$ /e$^-$Å^3	0.524, -0.562

Table 2. The average dipole moment (μ), the linear polarizability (α_0), the total polarizability (α_{tot}), and the first-order hyperpolarizability (β_{tot}) of **1** calculated at B3LYP/6-31+G(d,p)/LANL2DZ in gas phase.

Parameters*		Parameters*	
μ_x	-0.01	β_{xxx}	17.32

μ_y	2.97	β_{xxy}	1358.16
μ_z	0.74	β_{xyy}	-34.95
[1]μ (D)	**7.65**	β_{yyy}	6260.77
α_{xx}	470.07	β_{xxz}	37.18
α_{xy}	-2.67	β_{xyz}	131.06
α_{yy}	581.59	β_{yyz}	18.55
α_{xz}	-9.68	β_{xzz}	-5.98
α_{yz}	-0.35	β_{yzz}	-77.76
α_{zz}	171.30	β_{zzz}	21.36
[2]α_0	**407.65**		
[3]α_{tot} (esu)	**54.51x10^{-24}**	**[4]β_{tot} (esu)**	**62.28x10^{-30}**

*All values are given in a.u. unless otherwise stated.
(for α: 1 a.u.= 0.1482x10^{-24} esu; for β: 1 a.u.= 8.3693x10^{-33} esu)

[1] $\mu_{tot} = (\mu_x + \mu_y + \mu_z)^{1/2}$; [2] $\alpha_o = (\alpha_{xx} + \alpha_{yy} + \alpha_{zz})/3$;

[3] $\alpha_{tot} = 2^{-1/2}\left[\left(\alpha_{xx} - \alpha_{yy}\right)^2 + \left(\alpha_{yy} - \alpha_{zz}\right)^2 + \left(\alpha_{zz} - \alpha_{xx}\right)^2 + 6\alpha_{xz}^2\right]^{1/2}$;

[4] $\beta_{tot} = \left[\left(\beta_{xxx} + \beta_{xyy} + \beta_{xzz}\right)^2 + \left(\beta_{yyy} + \beta_{yzz} + \beta_{yxx}\right)^2 + \left(\beta_{zzz} + \beta_{zxx} + \beta_{zyy}\right)^2\right]^{1/2}$